

# Effective masses and complex dielectric function of cubic $HfO_2$

J. C. Garcia, L. M. R. Scolfaro, J. R. Leite, A. T. Lino

*Instituto de Física, Universidade de São Paulo,*

*C. P. 66318, 05315-970 São Paulo, SP, Brazil*

V. N. Freire, G. A. Farias

*Departamento de Física, Universidade Federal do Ceará,*

*C. P. 6030, 60455-900 Fortaleza, CE, Brazil*

E. F. da Silva Jr.

*Departamento de Física, Universidade Federal de Pernambuco, 50670-901 Recife, PE, Brazil*

(Dated: September 21, 2004)

## Abstract

The electronic band structure of cubic  $HfO_2$  is calculated using an *ab initio* all-electron self-consistent linear augmented plane-wave method, within the framework of the local-density approximation and taking into account full-relativistic contributions. From the band structure, the carrier effective masses and the complex dielectric function are obtained. The  $\Gamma$ -isotropic heavy and light electron effective masses are shown to be several times heavier than the electron tunneling effective mass measured recently. The imaginary part of the complex dielectric function  $\epsilon_2(\omega)$  is in good agreement with experimental data from ultraviolet spectroscopic ellipsometry measurements in bulk yttria-stabilized  $HfO_2$  as well as with those performed in films deposited with the tetrakis diethylamido hafnium precursor for energies smaller than 9.5 eV.

PACS[78.20.Ci, 71.18.+y,71.20.-b]

Contact author: scolfaro@macbeth.if.usp.br

Aggressive scaling of the gate lengths and equivalent gate oxide thickness following the *International Technology Roadmap for Semiconductors* (ITRS)<sup>1</sup> is forcing the replacement of silicon dioxide as a gate dielectric by high-dielectric constant (high- $\kappa$ ) materials to reduce leakage currents<sup>2</sup>, and meet requirements of reliability<sup>3</sup>. *Si*-related band offsets, permittivity, dielectric breakdown strength, interface stability and quality with silicon, and the carrier effective masses are key aspects of the new (high- $\kappa$ ) oxides that, together with costs of the fabrication processes<sup>4</sup>, have to be considered in extending Moore's law<sup>5</sup> to an equivalent oxide thickness below 10 nm.

Cubic hafnium oxide ( $HfO_2$ ) is an important candidate for  $SiO_2$  replacement as gate dielectric material. It has a dielectric constant  $\varepsilon_{HfO_2}(0) \simeq 25$  at 300 K, which is about six times higher than that of silicon dioxide, but more than an order of magnitude smaller than that of cubic  $SrTiO_3$ ,  $\varepsilon_{SrTiO_3}(0) \simeq 300$ , a competing high- $\kappa$  oxide. However,  $HfO_2$  has a conduction band offset  $\Delta E_{c,HfO_2} \sim 1.5 - 2.0$  eV with respect to silicon, which is more than one order of magnitude higher than that of cubic  $SrTiO_3$ ,  $\Delta E_{c,SrTiO_3} \sim 0.1$  eV<sup>6</sup>. The high dielectric constant and tunneling barrier (with respect to silicon) of  $HfO_2$ , together with a possible adaptation of the device production line to hafnium oxide thin film growth, make its candidate stronger for  $SiO_2$  replacement as gate dielectric material. Recently, improvements in the growth techniques of thin  $HfO_2$  films lead to a gate dielectric with 0.5 nm equivalent oxide thickness<sup>7</sup>.

A first-principles study of the structural, vibrational, and lattice dielectric properties of bulk hafnium oxide in the cubic, tetragonal, and monoclinic phases has been performed<sup>8</sup>, as well as a theoretical evaluation of some properties of thin  $HfO_2$  films on Si(001)<sup>9</sup>. However, few results concerning band-structure calculations have been published within the non-relativistic approach, or in the relativistic approach including spin-orbit interaction effects<sup>10-12</sup>. The values of the  $HfO_2$  carrier effective masses, which are fundamental to the modeling of tunneling currents through  $HfO_2$  gate dielectrics<sup>11,13</sup>, for example, have not been explicitly presented. State of the art full-relativistic calculations of the cubic  $HfO_2$  carrier effective masses and frequency-dependent dielectric function are presented in this work. The calculated  $\Gamma$ -isotropic heavy and light electron effective masses are several times heavier than the electron tunneling effective mass measured recently<sup>14,15</sup>. The calculated frequency behavior of the imaginary part of  $\varepsilon_{HfO_2}$  in the low energy range is in good agreement with the recent measurements of Lim *et al.*<sup>16</sup> by far ultraviolet (UV) spectroscopic

ellipsometry as well as with those of Edwards<sup>17</sup> and of Schaeffer *et al.*<sup>18</sup>.

The *ab initio* all-electron self-consistent linear augmented plane-wave (FLAPW) method, within the local-density functional formalism (LDA) and the generalized gradient approximation (GGA), is employed considering both non- and full-relativistic contributions to the band structure<sup>19</sup>. The 5s-, 5p-, 4f-, 5d-, 6s-Hf; 2s- and 2p-O electrons were treated as part of the valence-band states. Cubic fluorite-type HfO<sub>2</sub> belongs to the  $Fm\bar{3}m$  ( $Oh$ ) space (point) group, with Hf in (0,0,0), O in ( $\pm 1/4, \pm 1/4, \pm 1/4$ ), for which the Brillouin zone (BZ) is a 14 face polyhedral<sup>20,21</sup>. Through a total energy minimization process within GGA, a lattice constant  $a = 5.16 \text{ \AA}$  was obtained for cubic HfO<sub>2</sub>.

Our calculated value  $a_{min} = 5.16 \text{ \AA}$  is close to  $a = 5.06 \text{ \AA}$  and  $a = 5.04 \text{ \AA}$  obtained by Fiorentini and Gulleri<sup>9</sup> and Demkov<sup>10</sup>, respectively;  $a = 5.037 \text{ \AA}$  (LDA) and  $a = 5.248 \text{ \AA}$  (GGA) calculated by Zhao and Vanderbilt<sup>8</sup>. Note that the measured lattice constant  $a_{exp}$  is in the 5.08-5.30  $\text{\AA}$  range according to the data of Wang *et al.*<sup>21</sup>.

Figure 1 presents the band structure of cubic  $HfO_2$  along high-symmetry directions in the BZ and the total density of states (TDOS), which were calculated both in the non-relativistic (dashed lines) and relativistic (solid lines) approaches. The most relevant contributions of the relativistic corrections are due to the  $Hf(p)$ - and ( $d$ )-derived states, which contribute to the low energy pattern (between -10 and -18 eV) of the band structure. A remarkable shift, of  $\approx 6 \text{ eV}$  upwards is seen for the  $Hf(p)$ -derived states due to mass-velocity relativistic contributions. The upward shift of the  $Hf(p)$  states is followed by a spin-orbit splitting of about 2 eV which occurs between  $-10$  and  $-12 \text{ eV}$ . The top of the valence band is mostly of  $O(p)$  character with some mixture with the  $Hf(d)$ - as well as  $Hf(f)$ - derived states.  $HfO_2$  exhibits a direct gap at the  $X$ -point of  $3.65 \text{ eV}$ . Demkov<sup>10</sup> and Peacock and Robertson<sup>11</sup> obtained  $3.4 \text{ eV}$  using a plane wave basis set and nonlocal ultrasoft pseudopotentials (CASTEP code) within the LDA. Our value for the band gap energy is in good agreement with the value of  $3.6 \text{ eV}$  obtained by Boer and Groot<sup>12</sup> via LAPW-LDA calculations within a relativistic approach but not including spin-orbit interaction effects. All theoretical values for the band gap energy are smaller than experimental, which is due to the well-known underestimation of the energy values of conduction band states in *ab initio* calculations within the local-density functional theory. Through UV ellipsometry spectroscopy measurements in bulk yttria-stabilized  $HfO_2$  crystals Lim *et al.*<sup>16</sup> have assigned a value of  $\sim 5.8 \text{ eV}$  to the  $O(p) - Hf(d)$  band gap. We note that a value of  $3.29 \text{ eV}$  is obtained from the

non-relativistic calculation, and the band gap is of an indirect nature in this case.

Table I presents the carrier effective masses in the [100] and [111] ( $\Gamma \rightarrow L$ ,  $\Gamma \rightarrow X$ ,  $X \rightarrow \Gamma$ ) directions, calculated within and without (see the values in parenthesis) the full-relativistic approach. In the  $X \rightarrow W$  direction, the effective masses values are too high to be evaluated within a parabolic fit. In both the valence and conduction bands, the carrier effective masses are demonstrated to be highly anisotropic. Relativistic effects are seen to be mostly important in the  $\Gamma - L$  direction for electrons and holes, and in the  $\Gamma - X$  direction in the case of holes. The  $\Gamma$ -isotropic heavy and light electron effective masses, defined as  $m_{iso}^* = (8m_{\Gamma-L}^* + 6m_{\Gamma-X}^*)/14$ , have values  $m_{he}^* = 1.350 m_o$  and  $m_{le}^* = 0.714 m_o$ , respectively, where  $m_o$  is the free electron mass. Both  $m_{he}^*$  and  $m_{le}^*$  are several times heavier than the appropriately named tunnelling effective mass, which was recently estimated as:  $m_e^* = 0.1 m_o$ , through measurements of the temperature dependence of gate leakage current and Fowler-Nordheim tunnelling characteristics in metal/hafnium oxide/silicon structures<sup>14</sup>; and  $m_e^* = 0.17 m_o$ , through measurements of the direct tunnelling leakage current in  $n^+$  poly-Si gate NMOSFET with  $HfO_2$  as gate dielectric<sup>15</sup>. The severe discrepancy between the calculated  $\Gamma$ -isotropic electron effective masses and the experimental tunnelling effective mass in  $HfO_2$  highlights the limitations in taking the latter as a measure of the bulk  $HfO_2$   $\Gamma$ -isotropic electron effective mass. The large discrepancy may be related to the thin film characteristics and imperfections of the  $HfO_2$  gate dielectrics, as well as the influence of  $HfO_2/Si$  and  $HfO_2/metal$  interfaces on the gate current density in the devices. Measurements of the carrier effective masses in cubic  $HfO_2$  samples have not been performed yet, which precludes direct comparison of our theoretical estimates of the carrier effective masses with experiment.

The imaginary part,  $\epsilon_2(\omega)$ , of the complex dielectric function was obtained directly from full- and non-relativistic FLAPW electronic structure calculations, while the Kramers-Kronig relation was used to obtain the real part,  $\epsilon_1(\omega)$ . They are depicted in Fig. 2 over the energy range 0 – 16 eV. Relativistic contributions to the real and imaginary parts of the dielectric constant are found to be important, being responsible for a considerable shift of the main peaks towards higher energies. Moreover, due to the relativistic effects a more detailed structure is seen in particular for  $\epsilon_2(\omega)$ . Figure 3 shows good agreement of the calculated  $\epsilon_2(\omega)$  with the experimental data reported by Lim *et al.*<sup>16</sup> for energies smaller than 9.5 eV, and also with those performed by Edwards<sup>17</sup> and by Schaeffer *et al.*<sup>18</sup>, all using

UV ellipsometry spectroscopy. For this comparison the whole calculated spectrum for  $\epsilon_2$  was shifted to higher energies, by matching its energy threshold to the experimental value of the  $HfO_2$  gap energy.<sup>16</sup>

In conclusion, we have studied the band structure of cubic bulk  $HfO_2$  using first-principles calculations. Conduction- and valence-band effective masses were obtained and shown to be highly anisotropic. Relativistic effects are shown to play an important role, reflected in the effective mass values and in the detailed structure of the dielectric function. The  $\Gamma$ -isotropic heavy and light electron effective masses were determined to be several times heavier than the electron tunneling effective mass measured recently<sup>14,15</sup>. The calculated imaginary part of the dielectric function was shown to agree well with experimental measurements for energies smaller than 9.5 eV<sup>16-18</sup>.

The authors acknowledge the financial support received from FAPESP and the Brazilian National Research Council (CNPq) under contract NanoSemiMat/CNPq # 550.015/01-9. We thank Dr. A. Donegan for a critical reading of the manuscript.

- 
- <sup>1</sup> *International Technology Roadmap for Semiconductors: 2002* (Semiconductor Industry Association, San Jose, CA, 2002). See <http://public.itrs.net/>.
- <sup>2</sup> P. Packan, *Science* **285**, 2079 (1999); G. D. Wilk, R. M. Wallace, and J. M. Anthony, *J. Appl. Phys.* **89**, 5243 (2001), and references therein.
- <sup>3</sup> J. H. Stathis and D. J. DiMaria, *Microelec. Eng.* **48**, 395 (1999); D. A. Buchanan, *IBM J. Res. Develop.* **43**, 245 (1999); Y. C. Yeo, T. J. King, and C. M. Hu, *Appl. Phys. Lett.* **81**, 2091 (2002).
- <sup>4</sup> A. M. Stoneham, *J. Non-Cryst. Sol.* **303**, 114 (2002).
- <sup>5</sup> G. E. Moore, *Electronics* **83**, 114 (1965); *Proc. SPIE Int. Soc. Opt. Eng.* **2438**, 2 (1995).
- <sup>6</sup> V. V. Afanas'ev, A. Stesmans, F. Chen, X. Shi, S. A. Campbell, *Appl. Phys. Lett.* **81**, 1053 (2002).
- <sup>7</sup> H. Harris, K. Choi, N. Mehta, A. Chandolu, N. Biswas, G. Kipshidze, S. Nikishin, S. Gangopadhyay, and H. Temkin, *Appl. Phys. Lett.* **81**, 1065 (2002).
- <sup>8</sup> X. Zhao and D. Vanderbilt, *Phys. Rev. B* **65**, 233106 (2002).
- <sup>9</sup> V. Fiorentini and G. Gulleri, *Phys. Rev. Lett.* **89**, 6101 (2002).
- <sup>10</sup> A. A. Demkov, *Phys. Stat. Sol. (b)* **226**, 57 (2001).
- <sup>11</sup> P. W. Peacock and J. Robertson, *J. Appl. Phys.* **92**, 4712 (2002).
- <sup>12</sup> P. K. de Boer, and R. A. de Groot, *J. Phys. Cond. Matt.* **10**, 10241 (1998).
- <sup>13</sup> Y. T. Hou, M. F. Li, H. Y. Yu, D. L. Kwong, *IEEE Elect. Dev. Lett.* **24**, 96 (2003); Y. C. Yeo, T. J. King, and C. M. Hu, *J. Appl. Phys.* **92**, 7266 (2002).
- <sup>14</sup> W. J. Zhu, T.-P. Ma, T. Tamagawa, J. Kim, and Y. Di, *IEEE Elec. Dev. Lett* **23**, 97 (2002).
- <sup>15</sup> Y.-C. Yeo, T.-J. King, C. Hu, *Appl. Phys. Lett.* **81**, 2091 (2002).
- <sup>16</sup> S.-G. Lim, S. Kriventsov, T. N. Jackson, J. H. Haeni, D. G. Schlom, A. M. Balbashov, R. Uecker, P. Reiche, J. L. Freeouf, and G. Lucovsky, *J. Appl. Phys.* **91**, 4500 (2002).
- <sup>17</sup> N. V. Edwards, *AIP Conf. Proc.* **683** (1), 723 (2003).
- <sup>18</sup> J. Schaeffer, N. V. Edwards, R. Liu, D. Roan, B. Hradsky, R. Gregory, J. Kulik, E. Duda, L. Contreras, J. Christiansen, S. Zollner, P. Tobin, B. -Y. Nguyen, R. Nieh, M. Ramon, R. Rao, R. Hegde, R. Rai, J. Baker, and S. Voight, *J. Electrochemical Society* **150** (4), F67 (2003).
- <sup>19</sup> P. Blaha, K. Schwarz, P. Sorantin, and S. B. Trickey, *Comput. Phys. Commun.* **59**, 399 (1990);

K. Schwarz and P. Blaha, *Lecture Notes in Chemistry* **67**, 139 (1996).

<sup>20</sup> W. G. Wyckoff, *Crystal Structures*, V. 1, pp. 239-242 (John Wiley & Sons, New York, London, 1963).

<sup>21</sup> J. Wang, H. P. Li, and R. Stevens, *J. Mater. Sci.* **27**, 5397 (1992).

TABLE I: Valence- and conduction-band effective masses at relevant symmetry points in the BZ of  $HfO_2$ . Values are in units of the free electron mass,  $m_0$ . The numbers in parentheses correspond to effective-mass values obtained from a non-relativistic calculation.

k-direction	valence			conduction	
	$m_{hh}^*$	$m_{lh}^*$	$m_{so}^{*v}$	$m_{he}^*$	$m_{le}^*$
$\Gamma \rightarrow L$	0.871	0.580	0.720	0.930	0.823
	(0.815)	(0.657)	(...)	(0.781)	(0.781)
$\Gamma \rightarrow X$	9.9	0.338	0.710	1.91	0.570
	(8.327)	(0.240)	(...)	(2.017)	(0.493)
$X \rightarrow \Gamma$	0.286	...	...	1.268	...
	(0.268)	(...)	(...)	(1.832)	(...)



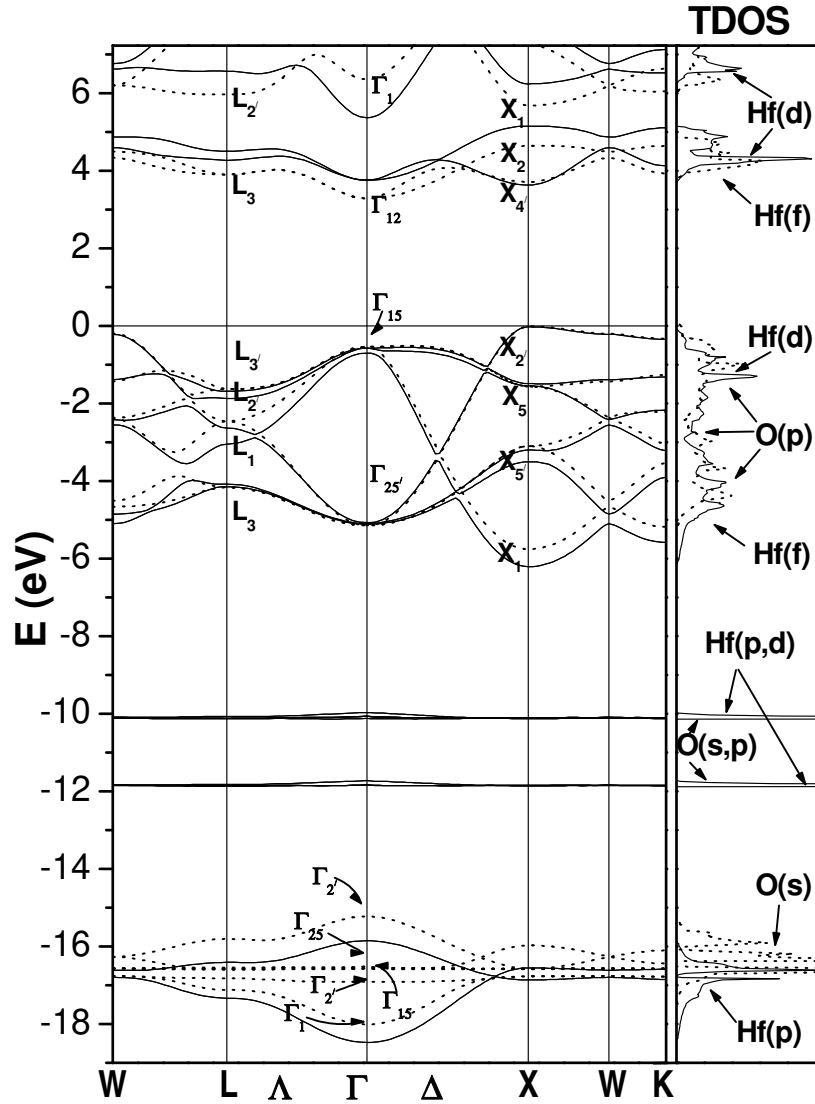


Fig.1

FIG. 1: Band structure of  $HfO_2$  along high-symmetry axis of the cubic BZ. The zero of energy (solid horizontal line) was set at the valence band maximum ( $X$ -point) for both, the full-relativistic and non-relativistic calculations. The total density of states (TDOS) is presented in the righthand column of the figure; the main contributions for the DOS peaks are depicted. Full-(non-) relativistic calculations are shown by solid (dashed) lines. High-symmetry points of some bands were labeled according to their irreducible representations given by group theory.

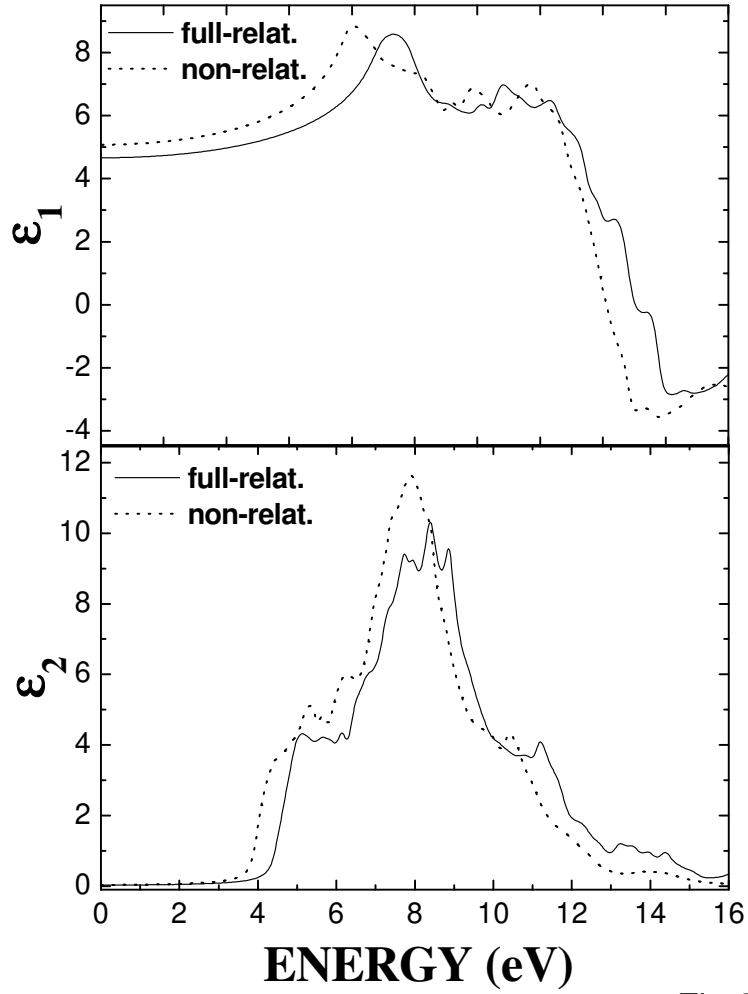


Fig.2

FIG. 2: Real ( $\epsilon_1$ ) and imaginary ( $\epsilon_2$ ) parts of the  $HfO_2$  complex dielectric function calculated within the full-relativistic (solid line) and non-relativistic (dashed line) approaches. The curves were plotted using a Lorentzian broadening of 0.1 eV.

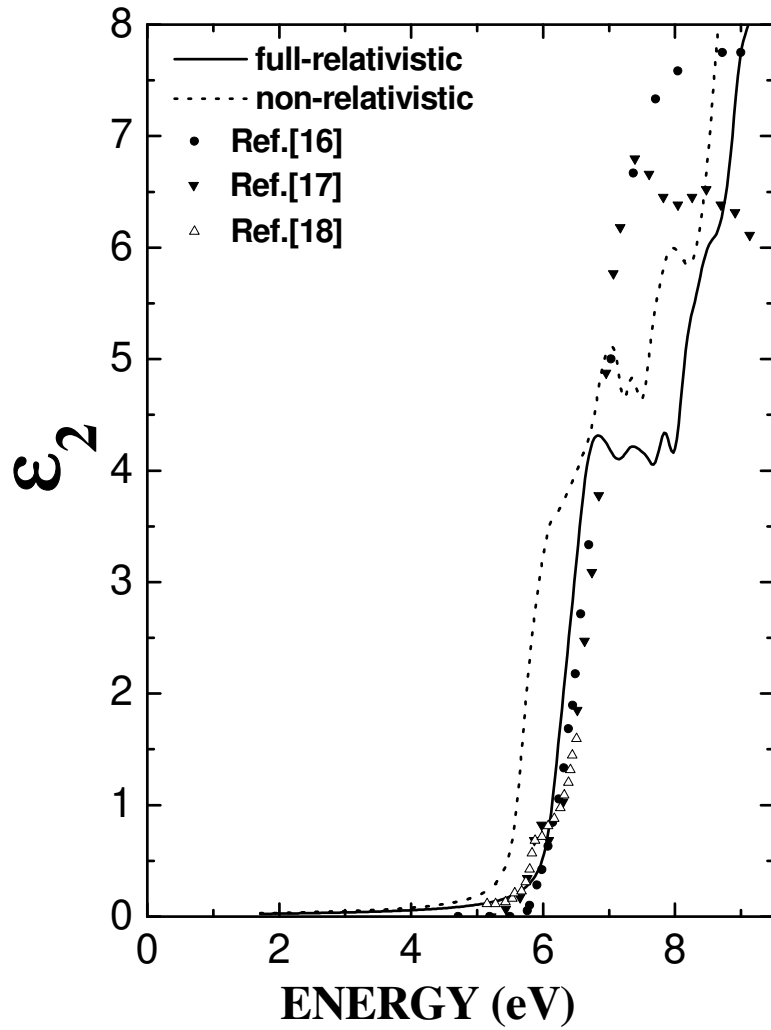


Fig.3

FIG. 3: Imaginary ( $\epsilon_2$ ) part of the  $HfO_2$  complex dielectric function calculated within the full-relativistic (solid line) and non-relativistic (dashed line) approaches. The calculated spectrum for  $\epsilon_2$  was shifted to higher energies, by matching its energy threshold to the experimental value of the  $HfO_2$  gap energy as obtained in Ref. [16]. The experimental data of Lim *et al.*<sup>16</sup> are depicted by full-dots, and those due to Edwards<sup>17</sup> and Schaeffer *et al.*<sup>18</sup> are depicted by upsidedown full-triangles and open-triangles, respectively.